Volume 10 | Issue 4 Article 2

Broken SU(3) Description Of Energy Levels And Decay Properties In Gadolinium Isotopes (A=156-160)

Fahmi Sh. Radhi
Mechanical Power Engineering Techniques Department, Shatt Al-Arab University College, Basra, Iraq,
dramir.ali53@gmail.com

Amir Abdul Ameer Mohammed Ali Dr.
Department of Radiology, College of Health and Medical Technology, University of Alkafeel,Najaf, Iraq,
dramir.ali53@gmail.com

Ali H. Al-Musawi
Department of Physics, College of Education for Pure Science, University of Kerbala, 56001 Karbala, Iraq

Follow this and additional works at: https://kijoms.uokerbala.edu.iq/home

 Part of the Biology Commons, Chemistry Commons, Computer Sciences Commons, and the Nuclear Commons

Recommended Citation

Radhi, Fahmi Sh.; Mohammed Ali, Amir Abdul Ameer Dr.; and Al-Musawi, Ali H. (2024) "Broken SU(3) Description Of Energy Levels And Decay Properties In Gadolinium Isotopes (A=156-160)," *Karbala International Journal of Modern Science*: Vol. 10 : Iss. 4 , Article 2.
Available at: https://doi.org/10.33640/2405-609X.3372

This Research Paper is brought to you for free and open access by Karbala International Journal of Modern Science. It has been accepted for inclusion in Karbala International Journal of Modern Science by an authorized editor of Karbala International Journal of Modern Science. For more information, please contact abdulateef1962@gmail.com.

University of Kerbala

Broken SU(3) Description Of Energy Levels And Decay Properties In Gadolinium Isotopes (A=156-160)

Abstract

This study presents an in-depth examination of the energy levels and decay properties of Gadolinium (Gd) isotopes with mass numbers (A=156-160), utilizing the Interacting Boson Model-1 (IBM-1) within a broken SU(3) symmetry framework. Through this approach, we systematically calculated and analyzed the energy spectra, B(E2) transition probabilities, quadrupole moments, and potential energy surface (PES) which provided valuable insights into the shape and collective behavior of nuclei, as well as the decay properties of the selected Gd isotopes. The broken SU(3) symmetries provide a good description to the isotopes under study. This comprehensive analysis enhances the understanding of the nuclear structure of mid-mass Gd isotopes, making valuable contributions to nuclear physics models and their predictive capabilities.

Keywords

Interacting boson model; quadrupole transition probabilities; broken SU(3) symmetry; potential energy surface

Creative Commons License

This work is licensed under a Creative Commons Attribution-Noncommercial-No Derivative Works 4.0 License.

Cover Page Footnote

Acknowledgment We would like to submit as authors to our universities that have contributed to supporting scientific research, as well as our families who helped us in completing the research, our appreciation and respect to everyone who contributed to helping us complete this research.

This research paper is available in Karbala International Journal of Modern Science: https://kijoms.uokerbala.edu.iq/home/vol10/iss4/2

REVIEW PAPER

Broken SU(3) Description of Energy Levels and Decay Properties in Gadolinium Isotopes (A=156−160)

Fahmi S. Radhi [a], Amir A. Mohammed Ali [b,*], Ali H. Al-Musawi [c]

[a] Mechanical Power Engineering Techniques Department, Shatt Al-Arab University College, Basra, Iraq
[b] Department of Radiology, College of Health and Medical Technology, University of Alkafeel, Najaf, Iraq
[c] Department of Physics, College of Education for Pure Science, University of Kerbala, 56001 Karbala, Iraq

Abstract

This study presents an in-depth examination of the energy levels and decay properties of Gadolinium (Gd) isotopes with mass numbers (A = 156−160), utilizing the Interacting Boson Model-1 (IBM-1) within a broken SU(3) symmetry framework. Through this approach, we systematically calculated and analyzed the energy spectra, B(E2) transition probabilities, quadrupole moments, and potential energy surface (PES) which provided valuable insights into the shape and collective behavior of nuclei, as well as the decay properties of the selected Gd isotopes. The broken SU(3) symmetries provide a good description to the isotopes under study. This comprehensive analysis enhances the understanding of the nuclear structure of mid-mass Gd isotopes, making valuable contributions to nuclear physics models and their predictive capabilities.

Keywords: Interacting boson model, Quadrupole transition probabilities, Broken SU(3) symmetry, Potential energy surface

1. Introduction

In nuclear physics, the structures and properties of atomic nuclei are described through various theoretical models and formalisms. Models such as the collective model [1], the shell model [2], the relativistic mean-field formalism [3], and others offer powerful tools for exploring and understanding these complex systems. Each model has its own strengths, and the choice of model typically depends on the specific properties or phenomena being investigated.

The region with atomic numbers Z ranging from 50 to 70 and mass numbers A between 150 and 170 is of considerable importance in nuclear physics, especially for concerning rare earth elements, lanthanides, and their isotopes, such as Samarium (Sm), Gadolinium (Gd), Dysprosium (Dy), and Erbium (Er) [4−8]. This area has been extensively studied, revealing intriguing phenomena related to nuclear structure, collective behavior, and fundamental interactions within atomic nuclei. The unique characteristics of these nuclei make them a central focus in both theoretical and experimental nuclear physics. The nuclei within this range have proton numbers that are relatively close to each other, with only a few units apart. This proximity in proton numbers places them in the same general region on the nuclear chart, resulting in similarities in their nuclear properties, and are all considered to be well-deformed, rotational nuclei. These elements have large quadrupole deformations, leading to pronounced rotational bands in their energy spectra.

The study of isotopes of (Gd), particularly in the mass range (A = 156−160), holds significant importance in nuclear physics. These isotopes lie in a region of the nuclear chart where complex phenomena such as shape coexistence, phase transitions, and the interplay between different modes of collective motion are prevalent. Understanding these isotopes provides critical insights into the

Received 23 June 2024; revised 9 September 2024; accepted 13 September 2024.
Available online 23 October 2024

* Corresponding author.
E-mail address: dramir.ali53@gmail.com (A.A. Mohammed Ali).

https://doi.org/10.33640/2405-609X.3372
2405-609X/© 2024 University of Kerbala. This is an open access article under the CC-BY-NC-ND license (http://creativecommons.org/licenses/by-nc-nd/4.0/).

behaviour of atomic nuclei under varying conditions of neutron and proton numbers. The neutron number plays a crucial role in determining the shape and structural transitions of Gd isotopes (Z = 64). As the neutron number changes in the isotopes, it affects the nuclear shape and the nature of collective excitations, as well as nuclei can exhibit shape coexistence, where different shapes (spherical, prolate, oblate) coexist at similar energy levels. Small changes in neutron number can shift the balance between these shapes, leading to sudden changes in the dominant shape of the nucleus. The study of low-lying excited states in Gd nuclei reveals significant information about the nuclear deformation and the collective behavior of these nuclei. The experimental data, coupled with theoretical models, help in understanding the interplay between collective rotational motion and single-particle excitations in these deformed nuclei.

The study of nuclear structure and properties, particularly in rare earth elements, provides vital insights into the underlying principles of nuclear physics. (Gd) isotopes, especially those with mass numbers ranging from (A = 156–160), are of significant interest because of their complex energy levels and decay properties. This research focuses on a detailed analysis of these isotopes using (IBM-1). As the neutron number crosses the closed shell at N = 82, the Gd nuclei exhibit increasing quadrupole deformation and are expected to be described by the SU(3) limit. Previous studies [6–14] have used various theoretical approaches to investigate the level structure of Gd isotopes.

LU Li-Jun [9] study the spectra and electromagnetic transition for the even-even $^{140-162}$Gd isotopes in the framework of the interacting boson model. A schematic Hamiltonian is used to describe the spectra and transitions. The results show that $^{140-162}$Gd are in the transition from the vibrational limit to the rotational limit. The properties of the low-energy electromagnetic dipole states in even–even $^{154-160}$Gd isotopes have been studied using the rotational, transitional and Galilean invariant Quasiparticle Random Phase approximation (QRPA) method [10].

Kassim [11] considered fully rotational (fully deformed) in ^{150}Ce, ^{152}Nd, ^{154}Sm, ^{156}Gd and ^{158}Dy nuclei when $R_{4/2}$ value ~ 3.33, and the shape phase transitions from U(5) to SU(3) in ^{148}Ba when $R_{4/2}$ value ~ 2.9. The energy levels, transition energy (E_γ) and B(E2) values were obtained for these isotopes using the IBM-1. The contour plot of PES shows that the shape phase transitions from U(5) to SU(3) for the ^{148}Ba, while ^{150}Ce,^{152}Nd,^{154}Sm, ^{156}Gd and ^{158}Dy nuclei are deformed and have rotational-like characteristics.

The positive ground-state band of $^{154-164}$Gd calculated using Bohr–Mottelson Model, Interacting Vector Boson Model and Interacting Boson Model, while the negative-parity band of $^{154-164}$Gd was calculated using Bohr–Mottelson Model and Interacting Vector Boson Model only. They adopted pure SU(3) symmetry in their calculations for band structure and transition probabilities [12].

The energies of low-lying levels and E2 transition rates for even Nd/Sm/Gd/Dy isotopes were calculated in the IBM framework and they applied a small perturbation in the SU(3) limit of the IBM was applied to these isotopes by adding n_d as a perturbation to the SU(3) Hamiltonian [13].

Leviatan [14] described level structure and calculated B(E2) values in the ^{156}Gd isotope using SU(3)-Partial dynamical symmetry (SU(3)-PDS). They identified several classes of (2 + 3)- body IBM Hamiltonians with SU(3) PDS and obtained an improved description of signature splitting in the γ - band of ^{156}Gd.

Raduta [15] utilized three versions of the coherent state model, namely CSM, CSM2, and GCSM, to describe the excitation energies and both intraband and interband transition probabilities of the ground, beta, and gamma bands in the even–even isotopes $^{150-160}$Gd. These nuclei were described in terms of U(5) to SU(3) symmetries, with ^{154}Gd displaying features specific to the X(5) symmetry. Radhi [16] described the ^{158}Gd in IBM-1 and IBM-2. They broke the SU(3) dynamical symmetry by introducing a value of pairing interaction, the degeneracy is lifted and the energy levels are brought up to the same order as the experimental ones. Khalaf [17] examined and described the geometric collective model and its application to nuclear shape transitions in Gd and Dy isotope chains. Their systematic studies on Gd/Dy chains revealed a shape transition from a spherical vibrator to an axially deformed rotor when moving from lighter to heavier isotopes.

In this work, we utilize an abundance of experimental data to calculate the positive-parity excited states and decay properties of the $^{156\text{-}160}$Gd isotopes beyond the ground state band using the SU(3) and broken SU(3) limits. Detailed analyses of energy levels, electric transition rates, and quadrupole moments are conducted and compared with the available experimental data. The phenomenon of back-bending is often observed, indicating a transition in the nuclear shape, such as from a more spherical to a more deformed shape, or vice versa, providing insights into the underlying structure of the nucleus. Furthermore, potential energy surfaces

(PES) for the isotopes of interest are computed and presented through contour plots. The concluding section summarizes the findings of this study.

2. Methodology

The IBM has become one of the most intensively used nuclear models [18,19], because of its ability to describe the changing low-lying collective properties of nuclei across an entire major shell with a simple Hamiltonian, and its ability to reproduce experimental data with relatively simple parameter fitting makes it a valuable approach alongside other methods such as the Nuclear Shell Model and Geometric Models. While each method has its strengths and limitations, IBM offers a balanced perspective that effectively captures the essence of nuclear collectively. In the IBM, the spectroscopies of low-lying collective properties of even-even nuclei [20] are described in terms of a system of interacting **s** bosons (**L=0**) and **d** bosons (**L=2**) [21]. Furthermore, the model assumes that the structure of low-lying levels is dominated by excitations among the valence particles outside major closed shells. In the particle space, the number of proton bosons N_π, and neutron bosons N_ν, are counted from the nearest closed shell, and the resulting total boson number is a strictly conserved quantity. The underlying structure of the six-dimensional unitary group SU(6) of the model [22] leads to a simple Hamiltonian, capable of describing the three specific types of collective structures with classical geometrical analogues (vibrational [23], rotational [24], and γ-unstable [25]) and transitional nuclei [26,27] whose structures are intermediate. In IBM-1, the Hamiltonian is written in terms of boson creation and boson annihilation operators. Thus [22],

$$H=\varepsilon_s(s^\dagger\tilde{s})+\varepsilon_d\sum_m d_m^\dagger\tilde{d}_m+V. \tag{1}$$

where ε_s, ε_d are the *s*- and *d*-boson energies, $s^\dagger$ ($\tilde{s}$), $d^\dagger(\tilde{d})$ are the creation (annihilation) operators for bosons in the $L=0$, $L=2$ states and V represents the boson-boson interactions.

The Hamiltonian can be expressed as [19]:

$$\begin{aligned}H=&\varepsilon_s(s^\dagger\cdot\hat{s})+\varepsilon_d(d^\dagger\cdot\hat{d})+\sum_{L=0,2,4}\frac{1}{2}(2L+1)^{1/2}C_L\left[[d^\dagger\times d^\dagger]^{(L)}\times[\hat{d}\times\hat{d}]^{(L)}\right]^{(0)}\\&+\frac{1}{\sqrt{2}}\hat{v}_2\left[[d^\dagger\times d^\dagger]^{(2)}\times[\hat{d}\times\hat{s}]^{(2)}+[d^\dagger\times s^\dagger]^{(2)}\times[\hat{d}\times\hat{d}]^{(2)}\right]^{(0)}\\&+\frac{1}{2}\hat{v}_0\left[[d^\dagger\times d^\dagger]^{(0)}\times[\hat{s}\times\hat{s}]^{(0)}+[s^\dagger\times s^\dagger]^{(0)}\times[\hat{d}\times\hat{d}]^{(0)}\right]\\&+u_2\left[[d^\dagger\times s^\dagger]^{(2)}\times[\hat{d}\times\hat{s}]^{(2)}\right]^{(0)}+\frac{1}{2}u_0\left[[s^\dagger\times s^\dagger]^{(0)}\times[\hat{s}\times\hat{s}]^{(0)}\right]^{(0)}.\end{aligned} \tag{2}$$

The most popular Hamiltonian H is given by Ref. [28]:

$$\begin{aligned}\hat{H}=&\varepsilon_d\hat{n}_d+a_0\hat{P}.\hat{P}+a_1\hat{L}.\hat{L}+a_2\hat{Q}.\hat{Q}+a_3\hat{T}_3.\hat{T}_3\\&+a_4\hat{T}_4.\hat{T}_4.\end{aligned} \tag{3}$$

where

$\hat{n}_d=(s^\dagger,d^\dagger)$ is the total number of d_{boson} operator,

$\hat{p}=1/2\,[(\hat{d}\cdot\hat{d})-(\hat{s}\cdot\hat{s})]$ is the pairing operator,

$\hat{L}=\sqrt{10}[d^\dagger\times\hat{d}]^1$ is the angular momentum operator,

$\hat{Q}=[d^\dagger\times\tilde{s}+s^\dagger\tilde{d}]^{(2)}-\frac{\sqrt{7}}{2}[d^\dagger\times\tilde{d}]^{(2)}$ is the quadrupole operator (χ is the quadrupole and take the values 0 *and* $\pm\frac{\sqrt{7}}{2}$),

$\hat{T}_r=[d^\dagger\times\hat{d}]^{(r)}$ is the octupole (r = 3) and hexadecapole (r = 4) operator, and

$\varepsilon=\varepsilon_s-\varepsilon_d$ is the boson energy.

The parameters a_0,a_1,a_2,a_3 *and* a_4 designate the strength of the pairing, angular momentum, quadrupole, octupole and hexadecapole interaction between the boson, respectively.

The three dynamical symmetries of the IBM model are expressed as follows [28]:

$$U(5):\hat{H}=\varepsilon\hat{n}_d+a_1\hat{L}.\hat{L}+a_3\hat{T}_3.\hat{T}_3+a_4\hat{T}_4.\hat{T}_4. \tag{4}$$

$$SU(3):\hat{H}=a_1\hat{L}.\hat{L}+a_2\hat{Q}.\hat{Q}. \tag{5}$$

$$O(6):\hat{H}=a_0\hat{P}.\hat{P}+a_1\hat{L}.\hat{L}+a_3\hat{T}_3.\hat{T}_3. \tag{6}$$

Another advantage of the interacting d-boson model is the matrix elements of the electric quadrupole operator. The reduced matrix elements of the E2 operator T(E2) have the form [19]:

$$T(E2)=\alpha_2[d^\dagger s+s^\dagger d]^{(2)}+\beta_2[d^\dagger d]^2. \tag{7}$$

where ($s^\dagger$, $d^\dagger$) and (s, d) are the creation and annihilation operators for s and d bosons, respectively, while α_2 and β_2 are two adjustable parameters that measure the strength of each term. The quadrupole moment for the $L=2^+$ state is defined as [22].

$$Q_{2_1^+} = \alpha_2 \sqrt{\frac{16\pi}{40}} \frac{2}{7}(4N+3). \quad (8)$$

3. Results and discussion

In IBM-1, the number of proton bosos (N_π) and neutron bosons (N_ν) is counted from the nearest closed shell without distinguishing between the particle and hole character of the pairs, and the resulting total boson number (N), $N = N_\pi + N_\nu$, is a strictly conserved quantity. The $^{156\text{-}160}$Gd isotopes have fourteen protons more than the magic number Z = 50, with neutron numbers N = 52 (away from the closed shell of N = 50), resulting in a total boson number N ranging from 12 to 14. The fundamental observable to describe dynamical symmetry of a specific nucleus is $R_{4/2}$ ratio, it has a value of 2.0 for the U (5) vibrational limit, 2.5 for the O (6) γ-unstable limit, and 3.33 for the SU (3) rotational limit. The experimental energy ratios R of the ^{156}Gd, ^{158}Gd, and ^{160}Gd isotopes are 3.237, 3.288, and 3.302, respectively [29–31], indicating that they have a rotational-like structure symmetry Table 1. As a result, the Hamiltonian of the SU(3) limit [28] given in Equation (5) is used in the calculations.

The energy eigenvalues of the SU(3) limit is given by Refs. [22,24]:

$$E|[N](\lambda,\mu)KLM\rangle = \frac{a_2}{2}\left(\lambda^2+\mu^2+\lambda\mu+3\lambda+3\mu\right) + \left(\frac{a_1-3a_2}{8}\right)L(L+1). \quad (9)$$

where $[N]$ labels the totally symmetric irreducible representations of SU(6), while (λ,μ) represents the SU(3) quantum number representations, and L refers to the eigenvalue of the total angular momentum. The values K and M correspond to the eigenvalues of the projection of the total angular momentum along the z-axis in the intrinsic frame and in the laboratory frame, respectively. The ground state band has a (2N, 0) representation. The γ and β bands belong to the (2N −4, 2) representations and correspond to the quantum numbers $K = 2$ and $K = 0$, respectively.

Table 1. The predicted R ratio in comparison with IBM limits and experimental values [29–31].

Isotopes	$E_{4_1^+}/E_{2_1^+}$		
	Exp.	*Broken SU(3*	*SU(3)*
$^{156}_{64}Gd$	3.236	3.333	3.325
$^{158}_{64}Gd$	3.304	3.324	3.341
$^{160}_{64}Gd$	3.307	3.319	3.333

Table 2. IBM-1 parameters (MeV) for $^{156\text{-}160}$Gd.

A	N	SU(3)[a]		Broken SU(3)[b]				CHQ
		ELL[a]	*QQ*[a]	*EPS*[b]	*PAIR*[b]	*ELL*[b]	*QQ*[b]	
156	12	0.0184	−0.0301	0.040	0.000	0.0160	−0.0305	−2.958
				0.000	0.0013	0.017	−0.0300	−2.958
158	13	0.0153	−0.0296	0.000	0.00328	0.0135	−0.0300	−2.958
160	14	0.0166	−0.0226	0.000	0.0170	0.0160	−0.0232	−2.958

EPS $= \varepsilon$, PAIR $= \frac{a_0}{2}$, ELL $= 2\,a_1$,Q.Q $= 2\,a_2$ and CHQ $= \sqrt{5}\,\chi$ are in the notations of PHINT program.
[a] Calculations I.
[b] Calculations II

3.1. Energy levels and reduced transition probabilities

The energy level calculations were carried out with PHINT code [32]. The strengths of interaction parameters a_1 and a_2 were evaluated from the relations given in Ref. [28]. The parameters used in the PHINT program are given in Table 2. The predicted energy levels are shown on the right side of Figs. 1–3. The rotational character of ground state bands is correctly reproduced by the SU(3) limit, but the spectrum contains degenerate β and γ bands. Furthermore, in the ^{158}Gd and ^{160}Gd isotopes, the β band is expected to be lower than the γ band. To account for the large difference between the experimental and predicted data, we perturbed the SU(3) symmetry by including a pairing interaction term. The Hamiltonian used in the calculations is [28]:

$$\widehat{H} = a_0 \widehat{p}.\widehat{p} + a_1\,\widehat{L}.\widehat{L} + a_2\,\widehat{Q}.\widehat{Q}. \quad (10)$$

Using the $SU(3) + \widehat{P}\widehat{P}$ interaction parameters, the predicted energy levels in the β and γ bands are

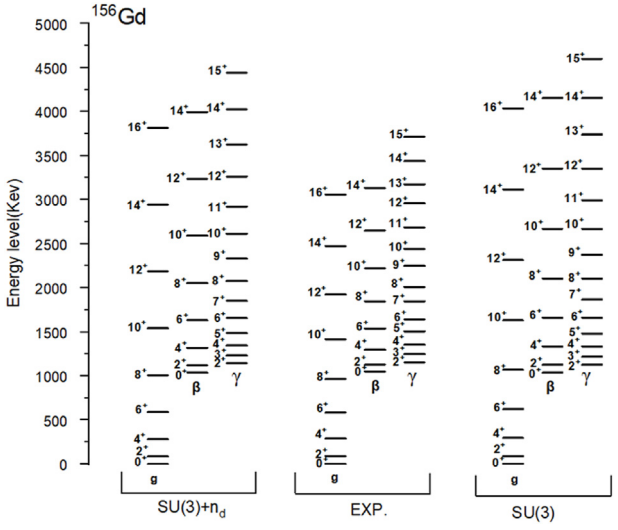

Fig. 1. ^{156}Gd experimental [29] energy levels compared with IBM-1 prediction (calculation II).

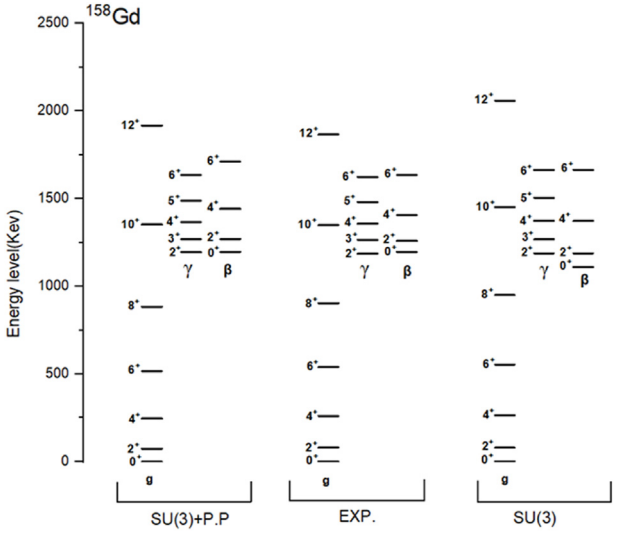

Fig. 2. ^{158}Gd experimental [30] energy levels compared with IBM-1 prediction.

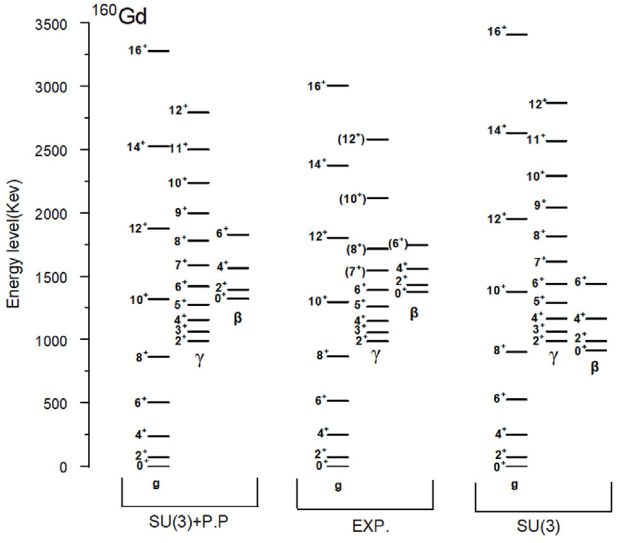

Fig. 3. ^{160}Gd experimental [31] energy levels compared with IBM-1 prediction.

accurately restored to their experimental counterparts, as shown on the left side of Figs. 2 and 3 This breaks the degenerate (λ-4,2) representation of the SU(3) limit, thereby removing energy state degeneracy.

However, while the pairing term was adequate to lift the degeneracy in the β and γ bands of the ^{156}Gd nucleus, the obtained wave function was not sufficient to produce a B(E2) value closer to the experimental value for most interband transitions (see Table 3 column 4). Instead of pairing, the n_d interaction term is used in the following Equation [28].

$$\widehat{H} = \varepsilon \widehat{n}_d + a_1 \widehat{L}.\widehat{L} + a_2 \widehat{Q}.\widehat{Q}. \tag{11}$$

Table 3. Parameters in (eb) of FBEM for B(E2) values calculation.

Isotope	SU(3)		Broken SU(3)	
	E2SD	E2DD	E2SD	E2DD
^{156}Gd	0.1200	−0.3549	0.1620	−0.0800
^{158}Gd	0.1185	−0.3505	0.1490	−0.1300
^{160}Gd	0.1093	−0.3225	0.1365	−0.1350

The predicted energy levels for ^{156}Gd, based on the broken SU(3) + n_d interaction parameters, are shown on the left side of Fig. 1. Table 2 displays the values of the fitted parameters. Figs. 1–3 compare the experimental spectra of the $^{156\text{-}160}$Gd isotopes [29–31] with the predictions of the SU(3) and broken SU(3) limits. The broken SU(3) limit provides a satisfactory description of the band structures in the $^{156\text{-}160}$Gd isotopes, calculating energy states that are closer to the experimental values than those predicted by the SU(3) limit. Levels denoted with "( )" indicate cases where the spin and parity of the corresponding states have not been experimentally established.

Fig. 4 shows the ground state band levels of the $^{156\text{-}160}$Gd isotopes. With increasing neutron number N, all levels appear to exhibit a smooth decrease in the energy value. The decrease in energy value of 2_1^+ and 4_1^+ states occur in a consistent proportion across all isotopes. This is reflected in the gradual increase in the R-ratio values when switching from one isotope to another, as shown in Fig. 5. The predicted R-ratio values in both limits differ slightly from the experimental value, but are identical to the standard IBM rotational value.

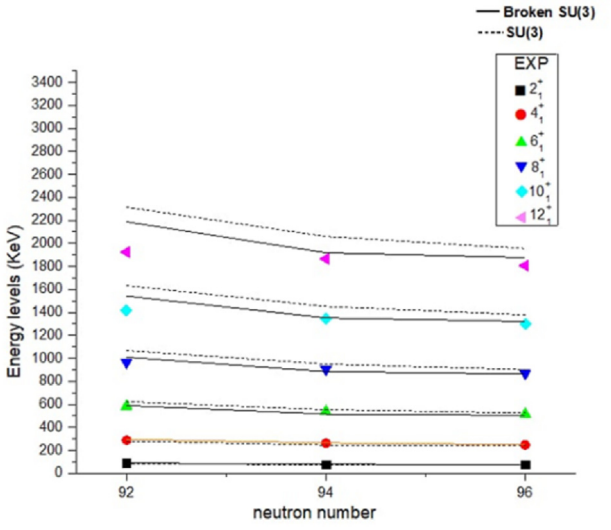

Fig. 4. Theoretical and experimental [29–31] ground state band energy levels of $^{156\text{-}160}$Gd isotopes as a function of N neutron number N.

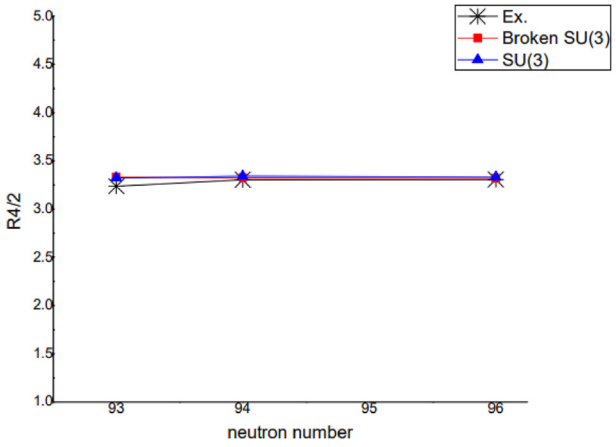

Fig. 5. The predicted R ratio in comparison with IBM limits and experimental values [29–31].

The E2 transitions provide a more rigorous test of the IBM model. In the IBM-1, the T_m operator takes the form [19]:

$$T_m^{(E2)} = \alpha_2[d^\dagger \times \tilde{s} + s^\dagger \times \tilde{d}]_m^{(2)} + \beta_2[d^\dagger \times \tilde{d}]_m^{(2)} \quad (12)$$

where α_2 and β_2 are the E2 multipolarity coefficients that measure the strength of each term. α_2 is the boson effective charge and β_2 is a parameter related to α_2. The wave function obtained from the diagonalization of the energy Hamiltonian is used in FBEM program [32] to account for reduced transition probabilities. The value of the boson effective charge α_2 can be calculated using the following formula for the SU(3) rotational limit [19].

$$B(E2; 2_1^+ \rightarrow 0_1^+) = \frac{\alpha_2^2}{5} N(2N+3) \quad (13)$$

The values of input parameters E2SD $= \alpha_2$ and E2DD $= \sqrt{5}\,\beta_2$ of Equation (10) were normalized to the experimental $B(E2: 2_1^+ \rightarrow 0_1^+)$ value and presented in Table 3. The predicted B(E2) values are shown in Table 4 column 3 and Table 5 columns 3 and 6. Intraband transitions exhibit noticeable B(E2) values, but B(E2) values for β→g and γ→g interband transitions are negligible.

In calculating the reduced transition probabilities using the broken SU(3) limit, the magnitude of the β/α ratio in the E2 operator Equation (10) deviates from the pure SU(3) symmetry value.

Consequently, the χ value in the E2DD parameter ranges from 0 to $\pm\sqrt{7}/2$, rather than the rotational limit. The newly fitted E2SD and E2DD values are presented in Table 3. When B(E2) values are calculated with the broken SU(3) limit, the β⟶g and γ⟶g interband transitions exhibit nonzero B(E2) values, as shown in columns 4 and 5 of Table 4, and columns 4 and 7 of Table 5. This is because the SU(3) B(E2) transition selection rule Δ(λ, μ) = 0 is no longer valid, allowing transitions between states of different representations are not prohibited. Tables 4 and 5 compare measured B(E2) values of $^{156\text{-}160}$Gd isotopes to IBM-1 predictions. We achieved the best fit for the β⟶g and γ⟶g interband transitions using the broken SU(3) limit, rather than the SU(3) limit, based on the available experimental data. The predicted B(E2) values from SU(3) + n_d are the closest to experimental values for ^{156}Gd among the three IBM-1 calculations shown in Table 4, and they also align well with results from Partial Dynamical Symmetry (SU(3)-PDS) [14]. The B(E2) ratio $R = (2_1^+ \rightarrow 0_1^+)/(4_1^+ \rightarrow 2_1^+)$, which is equal to1.4 in the rotational SU (3) limit [22] is a good indicator of nuclear collectively. Tables 4 and 5 show that the strength of B(E2) values increases with mass number for the $2_1^+ \rightarrow 0_1^+$ and $4_1^+ \rightarrow 2_1^+$ transitions, with the ratio R being 1.407, 1.409, and 1.411 for ^{156}Gd, ^{158}Gd, and ^{160}Gd, respectively. Furthermore, the IBM-1 determined electrical quadrupole moments Q_{2_1} correlate well with experimental results in both sign and magnitude for all considered isotopes. This explains the validity of the (IBM-1) in describing these isotopes. The success of the broken SU(3) limit indicates the necessity of considering deviations from pure SU(3) symmetry to accurately describe certain nuclei. This can provide insights into the shapes of these nuclei as prolate.

3.2. Back bending phenomenon

The active nucleons interacting with the core are considered the foundation of collective rotational motion in the nucleus. As is well known, the transition energy between yrast levels increases with angular momentum in the nuclei, but some nuclei appear to change abruptly [33,34]. The rotational energy can be calculated using this Equation [33,35].

$$\hbar\omega = \frac{E(L) - E(L-2)}{\sqrt{L(L+1)} - \sqrt{(L-2)(L-1)}}\,. \quad (14)$$

The transition energy and angular frequency of $^{156\text{-}160}$Gd isotopes are calculated according to SU(3) and broken SU(3) limits and compared to the measured data in Tables 6–8.

The angular frequency obtained from broken SU(3) symmetry agrees with experiment better than SU(3) symmetry. In terms of transition energy, the calculations showed good agreement with experimental data at $J = 8^+$ for ^{156}Gd and $J = 12^+$ for ^{158,160}Gd, with the broken SU(3) symmetry data being the closest to the experiment.

Table 4. Experimental $\mathbf{B(E2)(e^2b^2)}$ *values in* ^{156}Gd *compared with IBM-1 predictions.*

$J_i^+ \longrightarrow J_f^+$	*Exp. [29]*	IBM-1			SU(3)-*PDS* *[14]*
		SU(3)	*SU(3)+ P.P*	*SU(3)+ n_d*	
$2_g \longrightarrow 0_g$	0.9450(150)	0.9330	0.9217	0.9344	0.933
$4_g \longrightarrow 2_g$	1.3200(200)	1.3123	1.2963	1.3143	1.313
$6_g \longrightarrow 4_g$	1.4750(400)	1.4046	1.3873	1.4067	1.405
$8_g \longrightarrow 6_g$	1.6000(850)	1.4087	1.3910	1.4107	1.409
$10_g \longrightarrow 8_g$	1.57(7)	1.36	1.34	1.36	1.364
$12_g \longrightarrow 10_g$	1.50(2)	1.28	1.26	1.28	------
$14_g \longrightarrow 12_g$	------	1.1747	1.1587	1.1763	------
$16_g \longrightarrow 14_g$	------	1.0387	1.0240	1.0400	------
$0_\beta \longrightarrow 2_g$	$0.040(^{20}_{35})$	0.000	0.027	0.023	0.034
$2_\beta \longrightarrow 0_g$	0.0032(3)	0.000	0.030	0.003	0.0055
$2_\beta \longrightarrow 2_g$	0.0165(15)	0.0000	0.0490	0.0052	0.0084
$2_\beta \longrightarrow 4_g$	0.021(2)	0.0000	0.0033	0.0137	0.020
$2_\beta \longrightarrow 0_\beta$	0.260(115)	0.0040	0.0090	0.6877	0.679
$4_\beta \longrightarrow 2_g$	$0.0065(^{25}_{35})$	0.0000	0.0156	0.0049	0.0067
$4_\beta \longrightarrow 4_g$	-------	0.0000	0.0573	0.0034	0.0067
$4_\beta \longrightarrow 6_g$	$0.0105(^{35}_{55})$	0.0000	0.0084	0.0146	0.021
$4_\beta \longrightarrow 2_\beta$	$1.40(^{5}_{8})$	0.34	0.45	0.96	0.951
$2_\gamma \longrightarrow 0_g$	0.0234(8)	0.0000	0.0043	0.0322	0.030
$2_\gamma \longrightarrow 2_g$	0.0362(13)	0.0000	0.0070	0.0524	0.048
$2_\gamma \longrightarrow 4_g$	0.0038(2)	0.0000	0.0165	0.0034	0.0031
$3_\gamma \longrightarrow 2_g$	0.0365(7)	0.0000	0.0540	0.0568	0.053
$3_\gamma \longrightarrow 4_g$	0.0255(5)	0.0000	0.0284	0.0302	0.028
$4_\gamma \longrightarrow 2_g$	$0.009(^{2}_{3})$	0.0000	0.005	0.0153	0.015
$4_\gamma \longrightarrow 4_g$	$0.051(^{11}_{14})$	0.0000	0.01	0.062	0.057
$4_\gamma \longrightarrow 6_g$	-	0.0000	0.0164	0.0078	0.0076
$4_\gamma \longrightarrow 2_\beta$	$0.022(^{7}_{8})$	0.082	0.000	0.001	0.0096
$4_\gamma \longrightarrow 2_\gamma$	-	0.7638	0.9389	0.4617	-------
$5_\gamma \longrightarrow 4_g$	$0.040(^{115}_{25})$	0.0000	0.042	0.044	-------
$5_\gamma \longrightarrow 6_g$	$0.055(^{17}_{4})$	0.0000	0.037	0.0397	-------
$5_\gamma \longrightarrow 3_\gamma$	0.65(7)	0.66	0.71	0.73	-------
Q_{2_1}	-1.93(4)	-1.96	-1.94	-1.95	-------

The plot of transition energy as a function of spin is shown in Fig. 6. As angular momentum increases, the transition energy between yrast levels also increases, indicating the absence of the neutron pairing decoupling effect, which typically occurs outside the closed shell.

3.3. Potential energy surface

The potential energy surface (PES) in the nuclear physics represents the energy of a nucleus as a function of deformation parameters, typically denoted as β and γ. These parameters describe the shape of the nucleus, where β indicates the magnitude of deformation from a spherical shape and γ describes the axial asymmetry of the deformation. The PES calculations are carried out in conjunction with the intrinsic part of the IBM Hamiltonian, which is dependent on the shape variables β and γ. The (Gd) isotopes with mass numbers 156 to 160 are of interest due to their transitional behavior between spherical and deformed shapes. These isotopes provide a good testing ground for the IBM-1. The PES calculations are performed using the intrinsic part of the IBM Hamiltonian, which depends on the shape variable β and γ. The intrinsic ground state of the IBM-1 is defined by Ref. [28].

$$|N,\beta,\gamma\rangle = \mathbf{1}\Big/\sqrt{N!}\left(b_c^\dagger\right)^N|\mathbf{0}\rangle\,. \tag{15}$$

where N is the boson number, $|\mathbf{0}\rangle$ denotes the boson vacuum and $b_c^\dagger$ acts in the intrinsic system and given by Ref. [28]:

Table 5. Experimental $\mathbf{B(E2)(e^2b^2)}$ *values in* $^{158\text{-}160}$*Gd compared with IBM-1 prediction.*

$J_i^+ \rightarrow J_f^+$	^{158}Gd			^{160}Gd		
	Exp. [30]	*SU(3)*	*SU(3)+ PAIR*	*Exp. [31]*	*SU(3)*	*SU(3)+ PAIR*
$2_g \rightarrow 0_g$	1.0012(253)	1.0587	1.0132	1.0261(82)	1.0353	1.0337
$4_g \rightarrow 2_g$	1.4674(202)	1.4924	1.4280		1.4619	1.4590
$6_g \rightarrow 4_g$	-------	1.6040	1.5344	-	1.5764	1.5719
$8_g \rightarrow 6_g$	1.6698(152)	1.6189	1.5481	-	1.5991	1.5926
$10_g \rightarrow 8_g$	1.7204(152)	1.5820	1.5121	-	1.5739	1.5650
$12_g \rightarrow 10_g$	1.5686(152)	1.5086	1.4410	-	1.5155	1.5040
$14_g \rightarrow 12_g$				-	1.4305	1.4164
$16_g \rightarrow 14_g$				-	1.3221	1.3056
$2_\gamma \rightarrow 0_g$	0.0172(15)	0.0000	0.0208	0.0194(11)	0.0000	0.0197
$2_\gamma \rightarrow 2_g$	0.0303(35)	0.0000	0.0326	0.0362(10)	0.0000	0.0300
$2_\gamma \rightarrow 4_g$	0.0014(2)	0.0000	0.0021	0.0037(5)	0.0000	0.0018
$3_\gamma \rightarrow 2_g$	$0.0177(^{327}_{18})$	0.0000	0.0364		0.0000	0.0346
$3_\gamma \rightarrow 4_g$	$0.0090(^{165}_{10})$	0.0000	0.0186		0.0000	0.0165
$4_\gamma \rightarrow 2_g$	$0.0057(^{84}_{7})$	0.0000	0.0107	-	0.0000	0.0105
$4_\gamma \rightarrow 4_g$	$0.0369(^{54}_{45})$	0.0000	0.0384	-	0.0000	0.0355
$4_\gamma \rightarrow 6_g$	> 0.0048	0.0000	0.0053	-	0.0000	0.0044
$4_\gamma \rightarrow 2_\gamma$	$0.5717(^{8399}_{657})$	0.4879	0.5014	-	0.4880	0.5162
$5_\gamma \rightarrow 4_g$		0.0000	0.0290	-	0.0000	0.0283
$5_\gamma \rightarrow 6_g$		0.0000	0.0244	-	0.0000	0.0213
$5_\gamma \rightarrow 3_\gamma$		0.7774	0.7916	-	0.7766	0.8167
$6_\gamma \rightarrow 4_g$		0.0000	0.0075	-	0.0000	0.0078
$0_\beta \rightarrow 2_g$	$0.0059(^{212}_{7})$	0.0000	0.0158	-	0.0000	0.0040
$2_\beta \rightarrow 0_g$	0.0016(2)	0.0000	0.0025	-	0.0000	0.0007
$2_\beta \rightarrow 2_g$	0.0004(1)	0.0000	0.0040	-	0.0000	0.0010
$2_\beta \rightarrow 4_g$	0.0070(8)	0.0000	0.0093	-	0.0000	0.0023
$2_\beta \rightarrow 0_\beta$		0.8397	0.7661	-	0.7751	0.7945
$4_\beta \rightarrow 2_g$	$0.0066(^{134}_{10})$	0.0000	0.0030	-	0.0000	0.0008
$4_\beta \rightarrow 4_g$	$0.0019(^{37}_{3})$	0.0000	0.0037	-	0.0000	0.0010
$4_\beta \rightarrow 6_g$	$0.0159(^{319}_{23})$	0.0000	0.0091	-	0.0000	0.0022
$6_\beta \rightarrow 4_g$		0.0000	0.0026		0.0000	0.0007
Q_{2_1}	−2.01 (4)	-2.08	-2.03	-2.08(4)	-2.06	-2.05

Table 6. Comparison of experimental, SU(3), and broken SU(3) symmetry results for transition and rotational energies in ^{156}*Gd isotope [29].*

$J_f \rightarrow J_i$	E_γ(MeV) Exp.	$\hbar\omega$ (MeV) Exp.	E_γ(MeV) SU(3) + n_d	$\hbar\omega$ (MeV) SU(3) + n_d	E_γ(MeV) SU(3)	$\hbar\omega$ (MeV) SU(3)
$\mathbf{2_1^+ \rightarrow 0_1^+}$	**0.089**	**0.0363**	**0.084**	**0.034**	**0.089**	**0.036**
$\mathbf{4_1^+ \rightarrow 2_1^+}$	**0.199**	**0.0983**	**0.196**	**0.096**	**0.207**	**0.102**
$\mathbf{6_1^+ \rightarrow 4_1^+}$	**0.296**	**0.1473**	**0.308**	**0.153**	**0.327**	**0.162**
$\mathbf{8_1^+ \rightarrow 6_1^+}$	**0.381**	**0.1900**	**0.420**	**0.210**	**0.444**	**0.221**
$\mathbf{10_1^+ \rightarrow 8_1^+}$	**0.451**	**0.2251**	**0.533**	**0.266**	**0.564**	**0.281**
$\mathbf{12_1^+ \rightarrow 10_1^+}$	**0.508**	**0.2537**	**0.645**	**0.322**	**0.683**	**0.341**
$\mathbf{14_1^+ \rightarrow 12_1^+}$	**0.550**	**0.2753**	**0.757**	**0.378**	**0.802**	**0.403**
$\mathbf{16_1^+ \rightarrow 14_1^+}$	**0.584**	**0.2918**	**0.869**	**0.434**	**0.920**	**0.459**

$$b_c^\dagger = \frac{1}{\sqrt{1+\beta^2}}\left[s^\dagger + \beta\left(\cos\gamma\left(d_0^\dagger\right) + \frac{1}{\sqrt{2}}\sin\gamma\left(d_2^\dagger + d_{-2}^\dagger\right)\right)\right]. \tag{16}$$

The Potential Energy Surface (PES) associated with the IBM Hamiltonian of Equation (13) is given by Refs. [36–38]:

$$E(N,\beta,\gamma) = \frac{N}{1+\beta^2} + \frac{N(N-1)}{\left(1+\beta^2\right)^2}\left(A_1\beta^4 + A_2\beta^3\cos 3\gamma + A_3\beta^2 + A_4\right). \tag{17}$$

Where $A_i's$ are related to the coefficients C_L, υ_2, υ_0, u_2 and u_0 of Equation (2).

The energy functional corresponding to the three limits are given as [28,36–38]:

$$E(N,\beta,\gamma) = \varepsilon_d N\frac{\beta^2}{\left(1+\beta^2\right)}.\ \mathrm{U(5)} \tag{18}$$

$$E(N,\beta,\gamma) = \kappa N(N-1)\frac{1+\frac{3}{4}\beta^4 - \sqrt{2}\beta^3\cos 3\gamma}{\left(1+\beta^2\right)^2}.\ \mathrm{SU(3)} \tag{19}$$

Table 7. Comparison of experimental, SU(3), and broken SU(3) symmetry results for transition and rotational energies in ^{158}Gd [30].

$J_f \rightarrow J_i$	E_γ(MeV) Exp.	$\hbar\omega$ (MeV) Exp.	E_γ(MeV) SU(3) + n_d	$\hbar\omega$ (MeV) SU(3) + n_d	E_γ(MeV) SU(3)	$\hbar\omega$ (MeV) SU(3)
$2_1^+ \rightarrow 0_1^+$	0.079	0.0322	0.074	0.0302	0.079	0.0322
$4_1^+ \rightarrow 2_1^+$	0.182	0.0899	0.172	0.0850	0.185	0.0914
$6_1^+ \rightarrow 4_1^+$	0.278	0.1384	0.270	0.1344	0.290	0.1443
$8_1^+ \rightarrow 6_1^+$	0.365	0.1820	0.368	0.1835	0.396	0.1975
$10_1^+ \rightarrow 8_1^+$	0.445	0.2221	0.468	0.2336	0.502	0.2506
$12_1^+ \rightarrow 10_1^+$	0.516	0.2577	0.565	0.2822	0.607	0.3032

Table 8. Comparison of experimental, SU(3), and broken SU(3) symmetry results for transition and rotational energies in ^{160}Gd isotope [31].

$J_f \rightarrow J_i$	E_γ(MeV) Exp.	$\hbar\omega$ (MeV) Exp.	E_γ(MeV) SU(3) + n_d	$\hbar\omega$ (MeV) SU(3) + n_d	E_γ(MeV) SU(3)	$\hbar\omega$ (MeV) SU(3)
$2_1^+ \rightarrow 0_1^+$	0.075	0.030	0.072	0.029	0.075	0.0306
$4_1^+ \rightarrow 2_1^+$	0.173	0.085	0.167	0.082	0.175	0.0865
$6_1^+ \rightarrow 4_1^+$	0.267	0.132	0.256	0.131	0.276	0.1374
$8_1^+ \rightarrow 6_1^+$	0.353	0.176	0.360	0.179	0.376	0.1875
$10_1^+ \rightarrow 8_1^+$	0.432	0.215	0.457	0.228	0.476	0.2381
$12_1^+ \rightarrow 10_1^+$	0.506	0.252	0.555	0.277	0.576	0.2877
$14_1^+ \rightarrow 12_1^+$	0.571	0.285	0.652	0.325	0.676	0.3382
$16_1^+ \rightarrow 14_1^+$	0.631	0.315	0.750	0.375	0.778	0.3887

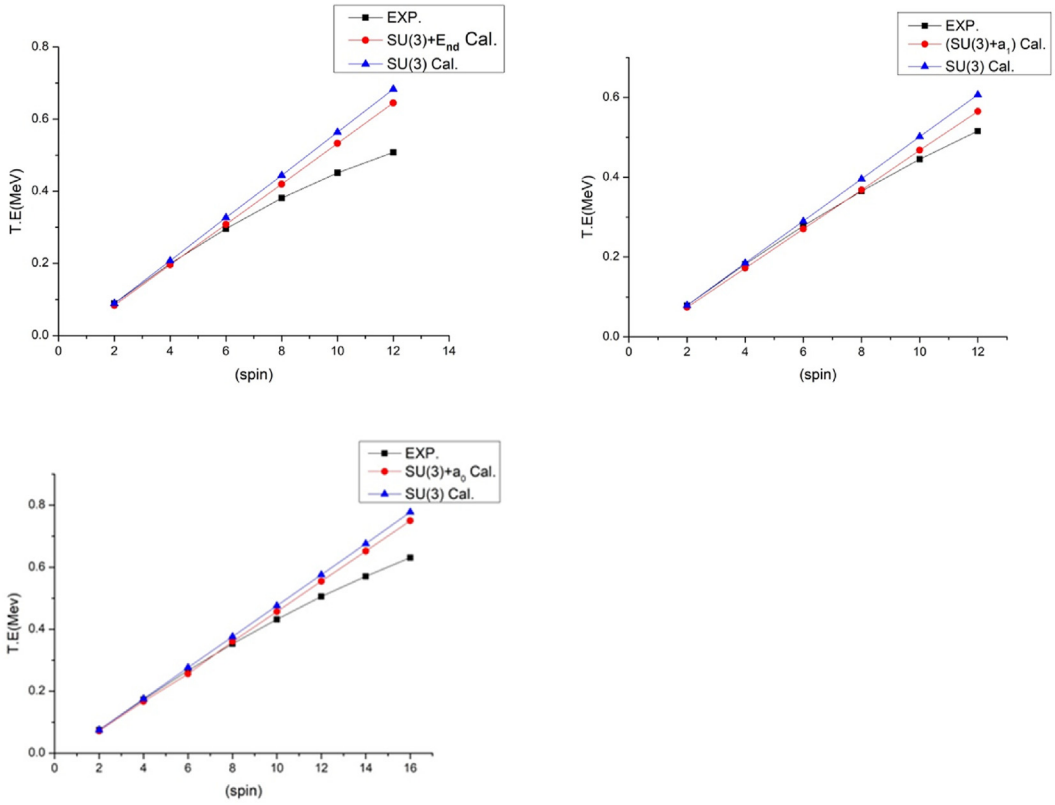

Fig. 6. Comparison of the calculated transition energy as a function of spin with the experimental for $^{156\text{-}160}$Gd [29–31].

$$E(N,\beta,\gamma) = \grave{\kappa} N(N-1)\left(\frac{1-\beta^2}{1+\beta^2}\right)^2 . \; O(6) \qquad (20)$$

Where $\kappa = -a_2/2$ *and* $\acute{\kappa} = -a_0$. The parameters β and γ define the geometry of the nuclear surface, with β taking values of $\beta \geq 0$ and γ ranging from 0 to π/3. The minimum values of β are $\beta_{min} = 0$ for U(5), $\sqrt{2}$ for SU(3), and 1 for O(6) [28]. When $\gamma = 0°$, the nucleus takes on a prolate shape, while at $\gamma = 60°$, it becomes oblate. Fig. 7 presents the contour plot of

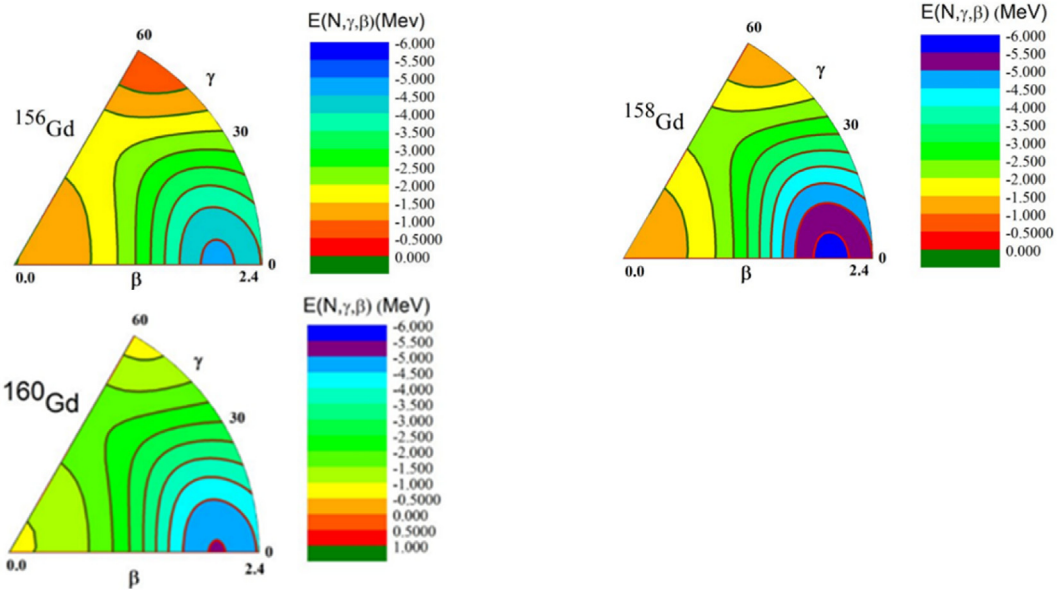

Fig. 7. The contour plots of potential energy surface for $^{156\text{-}160}$ Gd nuclei.

the (PESs) for the $^{156\text{-}160}$Gd isotopes, demonstrating that these isotopes are deformed and exhibit rotational like characters SU(3). Fig. 8 shows the PES plotted against $\gamma = 0^\circ$ and 60°, with $0 \leq \beta \leq 4$. The PES values for the $^{156\text{-}160}$Gd isotopes at $\gamma = 0^\circ$ are (-4.662, -5.654, and -5.0338 MeV) at $\beta =$ (1.4, 1.4 and 1.4) respectively, indicating a more pronounced prolate deformation compared to the oblate shape.

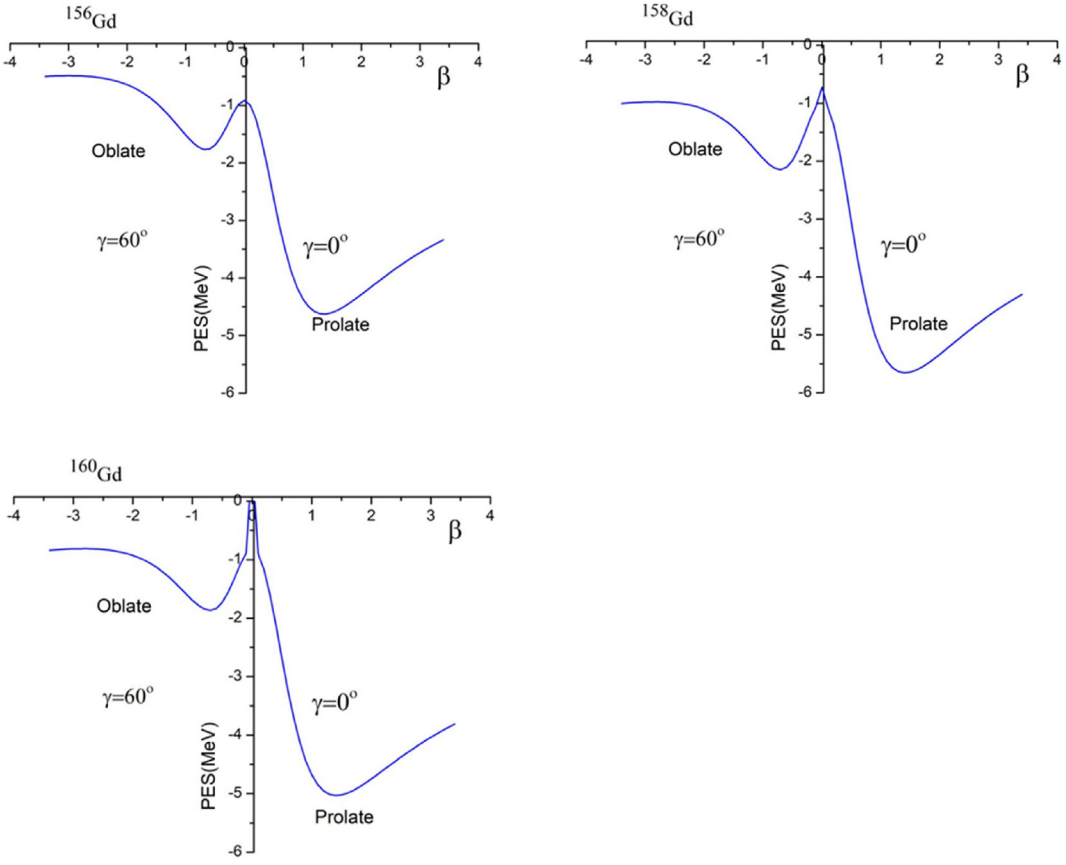

Fig. 8. The axial symmetric of the PESs for $^{156\text{-}160}$Gd isotopes.

4. Conclusion

This comprehensive study significantly enhances our understanding of the nuclear structure of mid-mass Gadolinium isotopes. The systematic calculations and analyses of the energy spectra, B(E2) transition probabilities, quadrupole moments, and potential energy surfaces (PES) have provided valuable insights into the shape and collective behavior of these nuclei. Initially, the SU(3) limit of the Interacting Boson Model (IBM) was applied to describe the isotopes $^{156\text{-}160}$Gd, which exhibit a rotational-like structure. This limit adequately describes the level structure of the ground state band. However, the energy levels and inter-band B(E2) transitions for the β and γ bands are not accurately reproduced using this limit alone. By breaking the SU(3) dynamical symmetry with a single interaction parameter, the predicted values for these properties align much more closely with the experimental results.

The calculations reveal that the n_d term with the SU(3) limit is an appropriate interaction parameter to study nuclei in the Gd region where the β-band is lower than the γ-band, as is the case for ^{156}Gd. Conversely, where the γ-band is lower than the β-band, the P.P term with the SU(3) limit is the best one to describe $^{158-160}$Gd. This approach is favored over the work of [9], which used a unique interaction term with the SU(3) limit for the $^{142-162}$Gd isotopic chain, describing all isotopes as U(5) ⟶ SU(3) transitional nuclei. The contour plot of the PES shows that the $^{156-160}$Gd nuclei are deformed and exhibit rotational-like characteristics.

The results of the current calculations for energy states and decay properties in the $^{156\text{-}160}$Gd isotopes show a strong agreement with experimental data. Additionally, these findings are consistent with the calculations from the SU(3)-Partial Dynamic Symmetry (SU(3)-PDS) model for the ^{156} Gd isotope, as referenced in Ref. [14]. This agreement indicates that our IBM-1 interaction parameters, which incorporate a broken SU(3) limit, are effective in describing the spectroscopic properties of the nuclides under study.

Ethics information

We certify that we have read the Journal's "Publication Ethics" shown on the link: https://kijoms.uokerbala.edu.iq/home/publication_ethics.html and we confirm that we follow strictly these "Publication Ethics".

We understand that the corresponding author is the sole contact for the Editorial process. The corresponding author is responsible for communicating with the other authors about progress, submissions of revisions and final approval of proofs.

Funding

This research was not funded by our universities, but by the authors.

Acknowledgment

We would like to submit as authors to our universities that have contributed to supporting scientific research, as well as our families who helped us in completing the research, our appreciation and respect to everyone who contributed to helping us complete this research.

References

[1] R.F. Casten, Nuclear structure from simple perspective, in: R. F. Casten, eds., Collective Excitations in Even-Even Nuclei, Vibrational and Rotational Motion, (2nd ed.), Oxford University Press. 2001, pp. 173–296, https://doi.org/10.1093/acprof:oso/9780198507246.003.0006.

[2] A. Gargano, G. De Gregorio, Realistic shell model and nuclei around ^{132}Sn, EPJA 20 (2003) 103–107, https://doi.org/10.1140/epja/i2002-10332-1.

[3] M. Bhuyan, S.K. Patra, P. Arumugam, Raj K. Gupta, Nuclear sub-structure in $^{112\text{-}122}$Ba nuclei within relativistic mean filed theory, IJMP E 20 (2011) 1227–1241, https://doi.org/10.1142/S021830131101837X.

[4] Amit Bindra, Sudden onset of deformation in A =150 mass nuclei, EJMCM 7 (2020) 3417–3419. https://ejmcm.com/uploads/paper/7f32c805459d2bf07b2397bf8530c602.pdf.

[5] Xiao-Tao He, L. Yu-Chun, Insight into nuclear midshell structures by studying K isomers in rare-earth neutron-rich nuclei, Phys. Rev. C 98 (2018) 064314, https://doi.org/10.1103/PhysRevC.98.064314.

[6] I. Bentley, S. Frauendorf, Microscopic calculation of interacting boson model parameters by potential-energy surface mapping, Phys. Rev. C 83 (2011) 064322, https://doi.org/10.1103/PhysRevC.83.064322.

[7] H.Y. Ji, G.L. Long, E.G. Zhao, S.W. Xu, Studies of the electric dipole transition of deformed rare-earth nuclei, Nucl. Phys. A 658 (1999) 197–216, https://doi.org/10.1016/S0375-9474(99)00335-8.

[8] A. Görgen, S. Siem, W. Korten, A. Obertelli, B. Sulignano, Ch Theisen, A. Bürger, M. Guttormsen, T.W. Hagen, A.C. Larsen, H.T. Nyhus, T. Renstrøm, N.U.H. Syed, H.K. Toft, G.M. Tveten, K. Wikan, J.P. Delaroche, M. Girod, J. Cederkäll, J. Van de Walle, E. Clément, G. De France, J. Ljungvall, P.A. Butler, M. Scheck, D.G. Jenkins, S. Freeman, P. Reiter, M. Seidlitz, A. Wendt, Study of oblate nuclear shapes and shape coexistence in neutron-deficient rare earth isotopes, in: Scientific Committee Paper, 2009. http://cds.cern.ch/record/1156116.

[9] Lu Li-Jun, Zhang Jin-Fu, Low-lying spectra and electromagnetic transition rates in $^{140-162}$Gd in the interacting boson model, CPC 30 (2006) 128–133. http://cpc.ihep.ac.cn/article/id/0d5fbd9c-c7c5-4bb0-923f-fb6520fd0a64.

[10] E. Guliyev, A. Kuliev, F. Ertugral, low-lying dipole excitations in the deformed even-even 154-160 Gd, Acta Physica Polonica B 40 (2009) 653–656. https://www.actaphys.uj.edu.pl/R/40/3/653.

[11] H.H. Kassim, Description of the Ba–Dy (N= 92) nuclei in the interacting boson model, Int. J. Mod. Phys. E 26 (2017) 1750019-13, https://doi.org/10.1142/S0218301317500197.

[12] M.A. Al-Jubbori, H.H. Kassim, F.I. Sharrad, A. Attarzadeh, I. Hossain, Theoretical description of the deformation

properties for 154–164Gd isotopes, Nucl. Phys. 970 (2018) 438–450, https://doi.org/10.1016/j.nuclphysa.2018.01.005.
[13] S.Y. Lee, J. Lee, Y.J. Lee, Calculations of the low-lying structures in the even-even Nd/Sm/Gd/Dy isotopes, JKPS 72 (2018) 1147–1151. https://link.springer.com/article/10.3938/jkps.72.1147.
[14] A. Leviatan, J.E. García-Ramos, P. Van Isacker, Partial dynamical symmetry as a selection criterion for many-body interactions, Phys. Rev. C 87 (2013) 021302-5, https://doi.org/10.1103/PhysRevC.87.021302.
[15] A. Raduta, A. Faessler, A coherent state description of the shape phase transition in even–even Gd isotopes, J. Phys. G: Nucl. Part. Phys. 31 (2005) 873–901. https://dio.org/10.1088/0954-3899/31/8/018.
[16] F. Radhi, H. Kassim, M.A. Al-Jubbori, I. Hossain, F.I. Sharrad, N. Aldahan, H.Y. Abdullah, Description of energy levels and decay properties in 158Gd nucleus, Nuclear Physics and Atomic Energy 24 (2023) 209–218, https://doi.org/10.15407/jnpae2023.03.209.
[17] A.M. Khalaf, H.F. Aly, A.A. Zaki, A.M. Ismail, Re-Examination of nuclear shape transitions in Gadolinium and Dysprosium isotopes chains by using the geometric collective model, progress in physics 10 (2014) 8–11. https://progress-in-physics.com/complete/PiP-2014-01.pdf.
[18] D. Janssen, R.V. Jolos, F. Dönau, An algebraic treatment of the nuclear quadrupole degree of freedom, Nucl. Phys. A 224 (1974) 93–115, https://doi.org/10.1016/0375-9474(74)90165-1.
[19] K. Abrahams, K. Allaart, A.E.L. Dieperink, Nuclear structure, in: F. Iachello, eds., An Introduction to the Interacting Boson Model, NATO Science Series B, 1981, pp. 53–89.
[20] E.A. McCutchan, N.V. Zamfir, R.F. Casten, Mapping the interacting boson approximation symmetry triangle: new trajectories of structural evolution of rare-earth nuclei, Phys. Rev. C 69 (2004) 064306, https://doi.org/10.1103/PhysRevC.69.064306.
[21] A. Arima, F. Iachello, Collective nuclear states as representations of a SU(6) group, Phys. Rev. Lett. 35 (1975) 1069, https://doi.org/10.1103/PhysRevLett.35.1069.
[22] F. Iachello, A. Arima, The Interacting Boson Model, Cambridge University Press, Cambridge. 1987, https://doi.org/10.1017/CBO9780511895517.
[23] A. Arima, F. Iachello, Interacting boson model of collective states I. The vibrational limit, Ann. Phys. (N. Y.) 99 (1976) 253–317, https://doi.org/10.1016/0003-4916(76)90097-X.
[24] A. Arima, F. Iachello, Interacting boson model of collective nuclear states II. The rotational limit, Ann. Phys. (N. Y.) 111 (1978) 201–238, https://doi.org/10.1016/0003-4916(78)90228-2.
[25] A. Arima, F. Iachello, Interacting boson model of collective nuclear states IV. The O(6) limit, Ann. Phys. (N. Y.) 123 (1979) 468–492, https://doi.org/10.1016/0003-4916(79)90347-6.
[26] O. Scholten, F. Iachello, A. Arima, Interacting boson model of collective nuclear states III. The transition from SU(5) to SU(3), Ann. Phys. NY 115 (1978) 325, https://doi.org/10.1016/0003-4916(78)90159-8.
[27] K. Nomura, Interacting boson model with energy density functionals, J. Phys.: Conf. Ser. 445 (2013) 012015. https://dio.or/10.1088/1742-6596/445/1/012015.
[28] R. Casten, D. Warner, The interacting boson approximation, Rev. Mod. Phys. 60 (1988) 389–469, https://doi.org/10.1103/RevModPhys.60.389.
[29] C. Reich, Nuclear data sheets for A= 156, Nucl. Data Sheets 113 (2012) 2537–2840, https://doi.org/10.1016/j.nds.2012.10.003.
[30] N. Nica, Nuclear data sheets for A= 158, Nucl. Data Sheets 141 (2017) 1–326, https://doi.org/10.1016/j.nds.2017.03.001.
[31]] N. Nica, Nuclear data sheets for A= 160, Nucl. Data Sheets 176 (2021) 1–428, https://doi.org/10.1016/j.nds.2021.08.001.
[32] O. Scholten, Computer Code PHINT, KVT, Groningen Holland. 1980.
[33] K.S. Krane, Introductory Nuclear Physics, John Wiley&Son Inc., New York. 1988.
[34] A.A. Mohammed-Ali, A.H.A. Al-Musawi, Study of the low-lying states in $^{142\text{-}144}$Ce isotopes using the IBM-1, in: AIP Conference Proceedings vol. 2290, 2020 050051. https://dio.org/10.1063/5.0028579.
[35] A. Castenholz, Algebraic Approaches to Nuclear Structure: Interacting Boson and Fermion Models (Contemporary Concepts in Physics), first ed., CRC Press. 1993.
[36] A. Arima, F. Iachello, The interacting boson model, Ann. Rev. Nucl. Part. Sci. 31 (1981) 75–105, https://doi.org/10.1146/annurev.ns.31.120181.000451.
[37] P. Van Isacker, Jin-Quan Chen, Classical limit of the interacting boson Hamiltonian, Phys. Rev. C 24 (1981) 684, https://doi.org/10.1103/PhysRevC.24.684.
[38] A.E.L. Dieperink, O. Scholten, F. Iachello, Classical limit of the interacting-boson model, Phys. Rev. Lett. 44 (1980) 1747, https://doi.org/10.1103/PhysRevLett.44.1747.